JMEPEG (2017) 26:3597–3606
DOI: 10.1007/s11665-017-2791-7

1059-9495/$19.00

Surface Characteristics of Machined NiTi Shape Memory Alloy: The Effects of Cryogenic Cooling and Preheating Conditions

Y. Kaynak, B. Huang, H.E. Karaca, and I.S. Jawahir

(Submitted November 14, 2016; in revised form April 28, 2017; published online June 20, 2017)

This experimental study focuses on the phase state and phase transformation response of the surface and subsurface of machined NiTi alloys. X-ray diffraction (XRD) analysis and differential scanning calorimeter techniques were utilized to measure the phase state and the transformation response of machined specimens, respectively. Specimens were machined under dry machining at ambient temperature, preheated conditions, and cryogenic cooling conditions at various cutting speeds. The findings from this research demonstrate that cryogenic machining substantially alters austenite finish temperature of martensitic NiTi alloy. Austenite finish (A_f) temperature shows more than 25 percent increase resulting from cryogenic machining compared with austenite finish temperature of as-received NiTi. Dry and preheated conditions do not substantially alter austenite finish temperature. XRD analysis shows that distinctive transformation from martensite to austenite occurs during machining process in all three conditions. Complete transformation from martensite to austenite is observed in dry cutting at all selected cutting speeds.

Keywords cryogenic machining, DSC analysis, NiTi shape memory alloy, surface integrity, XRD analysis

1. Introduction

Near-equiatomic NiTi shape memory alloys (SMAs) exhibit a reversible, diffusionless solid-to-solid-phase transformation from a high-temperature austenite phase to a low-temperature martensite phase (Ref 1). They possess a unique combination of properties including shape memory, superelasticity, great workability in the martensite state, and resistance to fatigue and corrosion (Ref 2). Thus, NiTi alloys have great potential for biomedical applications; therefore, these materials are being widely used in numerous biomedical applications (orthodontics, cardiovascular, orthopedics, urology, etc.) (Ref 3).

Considering biomedical applications, it is expected that NiTi alloys maintain their properties when they are subjected to repeatable large-strain bending deformations without permanent kinking (Ref 4). Namely, when they are subject to loading, they are expected to resist the functional fatigue failure that is induced from material processing and fabrication processes (Ref 5-7).

Conventional machining process and machining performance of NiTi alloys have been systematically investigated by researchers (Ref 8-10), and it is a well-known fact that machining processes induce an affected zone on the surface and subsurface of machined components, and this in turn effects the surface integrity characteristics of machined components. The magnitude and depth of the affected layer can be a function of different parameters; however, it is well established that the deformation temperature during the machining process plays a dominate role on the depth of the affected layer from the machined surface, and helps to determine whether the affected layer is thermally induced or mechanically induced. Consequently, machining conditions (cooling, and heating) and the cutting speed can be among the major parameters that need to be studied to understand their influence on the affected layer. It has been reported that due to machining processes and the resulting generated surface and subsurface characteristics, failure or functional fatigue can be determined in the medical components made from NiTi alloys (Ref 11). Considering these, investigating the effect of various machining conditions and cutting speed on transformation response of machined layer and the phase state after machining process would be appropriate and important. However, the machining research studies have in the past have generally focused on microhardness variation on the machined surface as a function of various inputs (Ref 10, 12, 13), and a few studies present limited DSC analysis by only focusing on dry versus online cryogenic cooling conditions in machining martensitic NiTi alloy (Ref 14, 15). Kaynak et al. (Ref 16, 17) presented machining-induced XRD analysis of austenitic NiTi alloys. It was reported that although at some machining conditions, martensite peaks were observed into XRD analysis, austenitic NiTi alloys does not show complete phase transformation resulting from machining (Ref 16, 17).

This study presents the results from an investigation of phase state and phase transformation response of martensitic NiTi alloys machined under dry, preheated, and cryogenic cooling conditions at various cutting speeds utilizing XRD and DSC analysis. Experimental findings illustrate that austenite

Y. Kaynak, Department of Mechanical Engineering, Faculty of Technology, Marmara University, Goztepe Campus, Kadikoy, 34722 Istanbul, Turkey, **B. Huang** and **I.S. Jawahir**, Department of Mechanical Engineering, College of Engineering, University of Kentucky, Lexington, KY 40506; and Institute for Sustainable Manufacturing (ISM), University of Kentucky, Lexington, KY 40506; and **H.E. Karaca**, Department of Mechanical Engineering, College of Engineering, University of Kentucky, Lexington, KY 40506. Contact e-mails: yusuf.kaynak@marmara.edu.tr and yusuf_kaynak@yahoo.com.

finish temperature of martensitic NiTi alloy is increased more than 25 percent resulting from cryogenic machining. XRD analysis shows that phase transformation takes place in all three conditions. Besides, complete transformation is also observed in dry machining at all cutting speeds and in preheated conditions at some cutting speeds.

2. Experimental Work

2.1 Work Material

The material used in this study was a commercially available, $Ni_{49.9}Ti_{50.1}$ (at.%) alloy. The material was received as round bars with a diameter of 10 mm in a hot-rolled/hot-drawn and hot-straightened condition. The alloy is single phase, with a dynamically recrystallized and equiaxed grain structure with approximately 20-30 μm average grain size (Ref 18), as shown in Fig. 1. The NiTi alloy was in its martensitic phase at room temperature as determined by PerkinElmer differential scanning calorimetry (DSC) where the martensite start, martensite finish, austenite start, and austenite finish temperatures are 73, 49, 86, and 107 °C, respectively, as shown in Fig. 2.

2.2 Cutting Tool, Cutting Parameters, and Cooling/Heating Conditions

DCGT 11T308HP grade KC5410 cutting tool inserts with TiB_2 coating were used in all machining experiments. The edge radius of the tools varied between 18 and 20 μm. It should be noted that this selected insert with coating is the most commonly recommended tool type for turning of NiTi shape memory alloys (Ref 9). The tool holder was SDJCL 12 3B H5 M. During all machining trials, the feed rate, f, and depth of cut, d, were kept constant at 0.05 mm/rev and 0.5 mm, respectively. The only machining variable, other than the cooling/heating environment, that was changed was cutting speed, V, which was varied from 12.5 to 100 m/min. At each cutting speed, samples were machined under three different conditions: (i) machined dry at ambient temperature, (ii) machined dry at a preheated temperature of 175 °C, and (iii) machined cryogenically using liquid nitrogen.

In the cryogenic machining process, liquid nitrogen was delivered to the cutting region through two 4.78 mm diameter nozzles applied under 1.5 MPa pressure with 10 g/s mass flow rate. One of the nozzles was placed at the rake face, and the other nozzle was placed at the flank face of the cutting tool (Ref 9).

The DMP CryoTemper chamber was used for preheating the workpieces. In this case, samples were heated at 175 °C for 30 min, followed immediately by the cutting process under dry conditions. The DSC results (Fig. 2) confirm that the material is fully austenitic (B2 crystal structure) at 175 °C so that the entire machining process is performed in the austenitic condition. Samples were also machined dry under ambient conditions. At room temperature, the workpiece is completely B19′ martensite prior to the start of machining (Fig. 2), but as described below, the "ambient" condition of the workpiece quickly changes with the onset of machining.

2.3 Measurements

In this study, XRD and DSC responses of machined $Ni_{49.9}Ti_{50.1}$ alloys are the two considered main outputs. For observing the phase state of as-received and machined samples of NiTi alloys, BrukerD8 Discover x-ray diffractometer with a quarter Eulerian cradle which integrates phi and chi rotations was used. The x-ray diffraction patterns were measured using CuK_α radiation ($\lambda = 1.5406$ Å nm, $K\alpha1/K\alpha2 = 0.5$) from a source operated at 40 kV and 44 mA. The round bar samples were positioned at the center of the x-ray goniometer. XRD spectra of machined NiTi samples were carried out from 35° to 55° at room temperature. The scan speed was 1.5°/min.

XRD peak positions and the corresponding 2θ degrees were found using lattice parameters $a = 0.291$ nm, $b = 0.414$ nm, $c = 0.467$ nm and $\beta = 97.55°$ (Ref 19) for martensite (B19′) and $a = 3015$ nm for austenite phase (B2) (Ref 20). XRD pattern of the as-received NiTi alloy is presented in Fig. 4.

The characterization of machining-induced phase transformation of the surface and subsurface of the machined samples was made by using a PerkinElmer DSC at a heating and cooling rate of 10 °C min^{-1}. DSC samples were cut using a slow-speed diamond saw from the surface/subsurface region of the machined samples as schematically illustrated in Fig. 3. The locations where the DSC samples were cut from machined

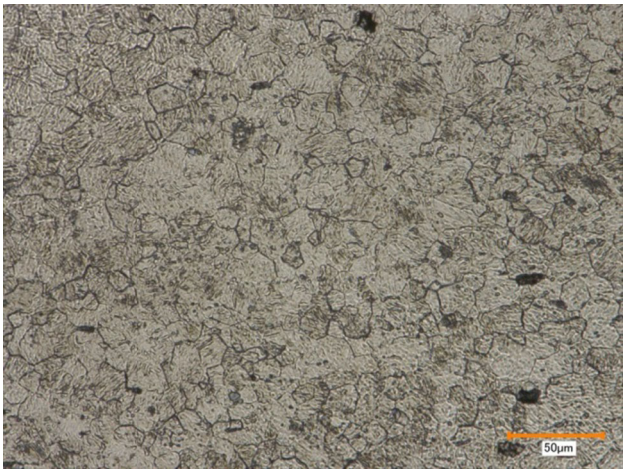

Fig. 1 Phase transformation temperature and typical microstructure of NiTi SMAs

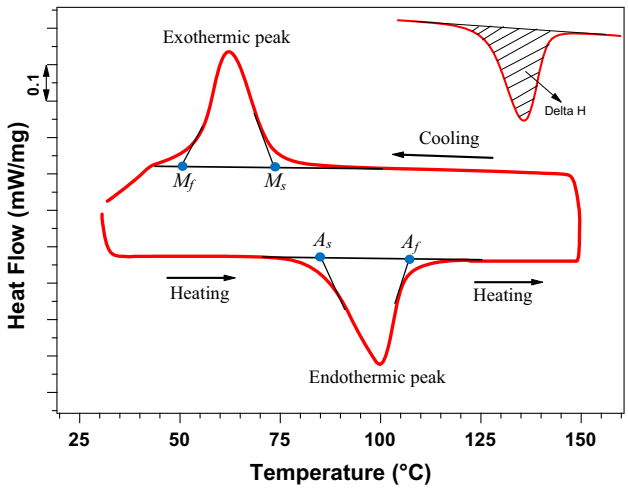

Fig. 2 DSC results of as-received $Ni_{49.9}Ti_{50.1}$ alloy

samples are also schematically presented in Fig. 3. The thickness of samples was approximately 300 μm after mechanical polishing. To eliminate the effect of blade cutting, the samples were mechanically polished using 800-grit SiC papers prior to DSC analysis. The measured phase transformation temperature of as-received $Ni_{49.9}Ti_{50.1}$ alloys is presented in Fig. 2.

3. Results and Discussion

3.1 Phase Transformation Analysis

$Ni_{49.9}Ti_{50.1}$ alloys have a relatively low phase transformation temperature in comparison with other engineering materials. During the machining process without active cooling systems, the temperature of work material exceeds the transformation temperatures of $Ni_{49.9}Ti_{50.1}$ alloys (Ref 19). Consequently, it is expected that the work material undergoes reverse phase transformation from martensite to austenite ($M \rightarrow A$). As the temperature of the work material decreases down to room temperature, forward transformation ($A \rightarrow M$) takes place after cutting process. However, during the cutting process, generated stress, increased dislocation density can lead to suppressing the forward transformation on the surface and subsurface. Moreover, during the cutting process, work material is also subjected to mechanical load that influences the shape memory response by increasing the transformation temperatures of the $Ni_{49.9}Ti_{50.1}$ work material. In this study, the role of thermal and mechanical effects on the phase state of work material is investigated.

Figure 4 shows the effect of various machining processes on the XRD spectra of the surfaces of machined $Ni_{49.9}Ti_{50.1}$ samples at low cutting speed of 12.5 m/min. It also shows XRD spectra of the as-received material. As-received material does not have any austenite peak, as shown in Fig. 4. But all machined NiTi alloy has austenite peak that should be noted. Surface layer of dry and preheated machined samples transformed from martensite to austenite phase. In the cryogenically machined sample, peak broadening occurs and existing phases cannot clearly be determined. However, it is also possible to assume that these peaks indicate martensitic phases.

The XRD response of machined samples at high cutting speed of $V = 100$ m/min are shown in Fig. 5. Higher cutting speeds indicate that the $Ni_{49.9}Ti_{50.1}$ is subjected to higher temperatures during the machining process (Ref 21). Although as-received sample is in martensite phase at room temperature, all three machined samples have distinctive austenitic peaks. Thus, at higher cutting speed, martensite to austenite transformation takes place. However, the heavy deformation of samples can be partially annihilated at higher cutting speed as the temperature increases. Consequently, peak broadening in cryogenically machined sample at high speed is not as pronounced as the one at low speed and austenite peak can easily be determined. Thus, we can conclude that the cutting temperature plays a major role on surface phase state of machined $Ni_{49.9}Ti_{50.1}$ alloys.

These findings are very helpful for the understanding the effect of machining on the surface and subsurface phase state of components. Phase transformation can be clearly seen in all conditions. In literature, XRD analysis of various machined materials including Ti-6Al-4V, steel and Inconel 718 were presented (Ref 22-25) These studies reported peak shifting and peak broadening as main findings (Ref 22-25) without complete phase transformation (Ref 22-25). Previously, partial phase transformation (observing both martensite and austenite peaks with XRD analysis) was reported after machining of austenitic NiTi alloys, (Ref 16, 17). The current study illustrates that in dry machining and some cases of preheated cutting, complete phase transformation (observing only austenite phase) can be observed in NiTi alloys.

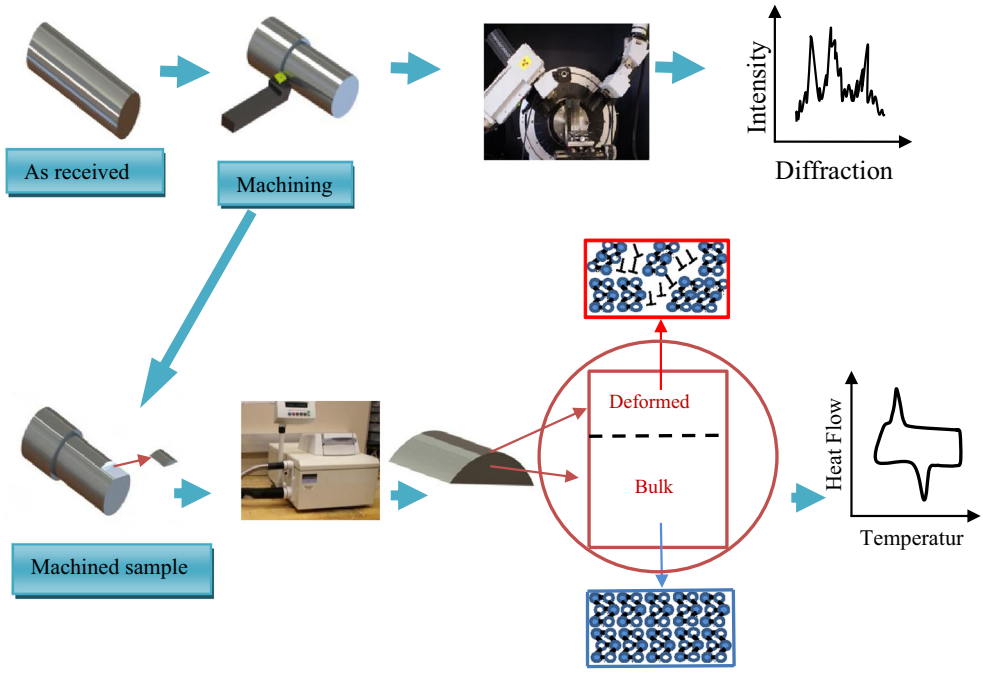

Fig. 3 Schematic representation of experimental processes and measurements

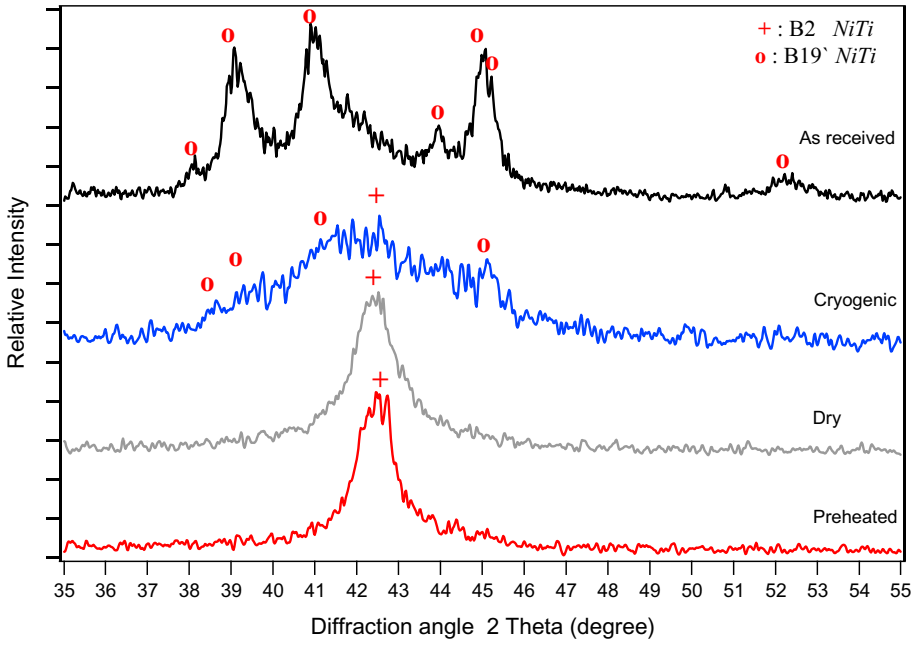

Fig. 4 Comparison of XRD patterns of $Ni_{49.9}Ti_{50.1}$ alloys after machining at 12.5 m/min

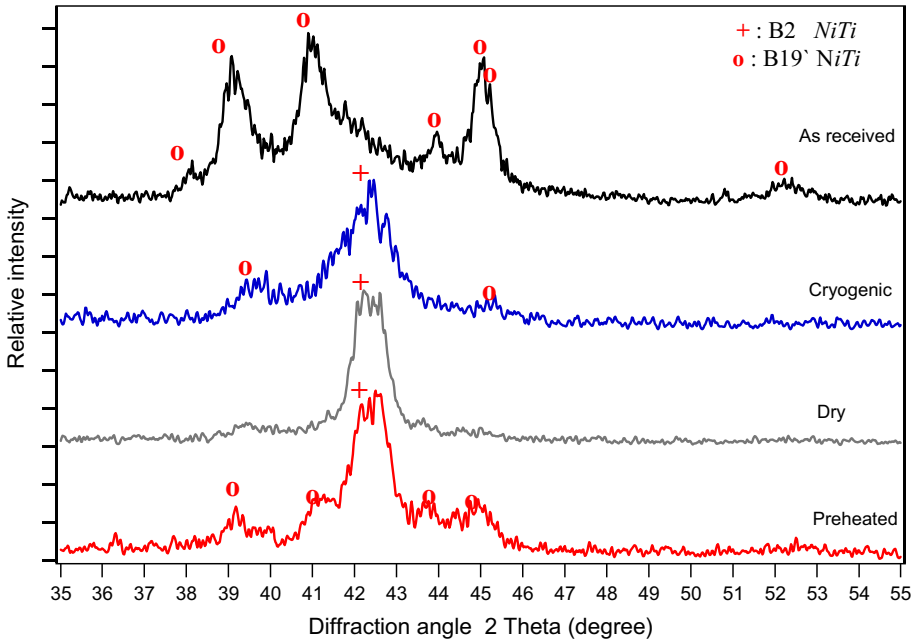

Fig. 5 Comparison of XRD patterns of $Ni_{49.9}Ti_{50.1}$ alloys after machining at 100 m/min

Figure 6 shows XRD patterns of machined samples under dry cutting at selected cutting speeds from 12.5 to 100 m/min. The surfaces of all the machined samples are austenite. It should also be noted that at lower cutting speeds, the austenite peak is broader as compared to higher cutting speeds. In dry cutting conditions, the cutting temperature easily exceeds transformation temperatures of $Ni_{49.9}Ti_{50.1}$ alloys, and thus deformation takes place when the material is in austenite state. After machining process is completed, the deformed structure does not allow the surface and subsurface to transform back to martensite despite cooling the sample below the M_f of as-received material. As cutting speed increases, temperature increases, and in turn mechanical effects get smaller due to dislocation annihilation. Therefore, at higher cutting speeds, the peak does not broaden as much as it does at low speeds.

Figure 7 shows XRD patterns of machined samples under preheated cutting conditions at selected cutting speeds. Although the austenitic peak's broadening does not change, martensitic peaks can be clearly seen in preheated machining. When the material is heated to 175 °C (above A_f) for machining, the material transforms from martensite to austenite. During the cutting process, temperature increases more and thus reduces the density of dislocation and defects in the machined surface. After the cutting process, as the work

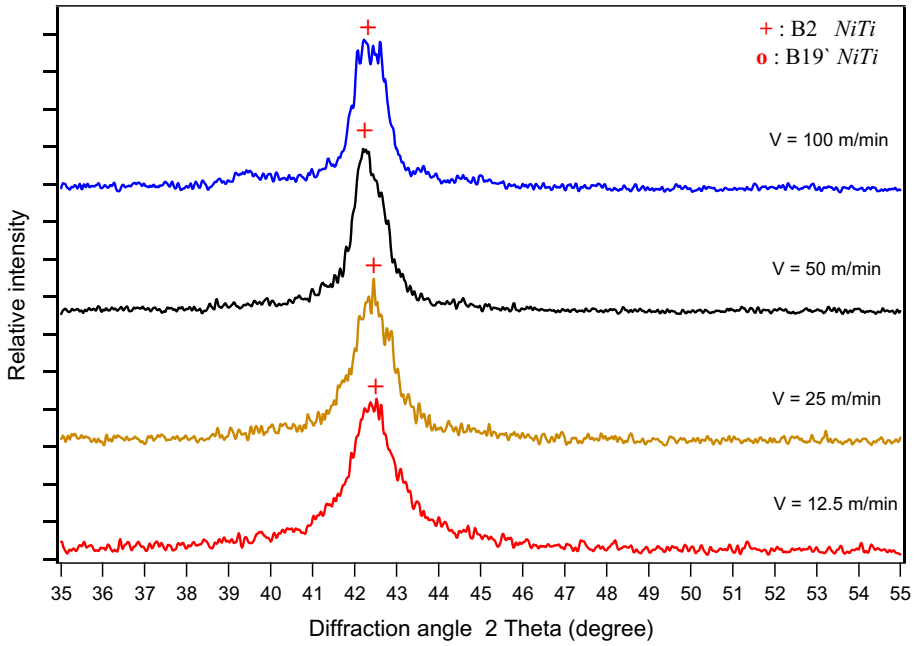

Fig. 6 XRD patterns of dry machined $Ni_{49.9}Ti_{50.1}$ SMAs at selected cutting speeds

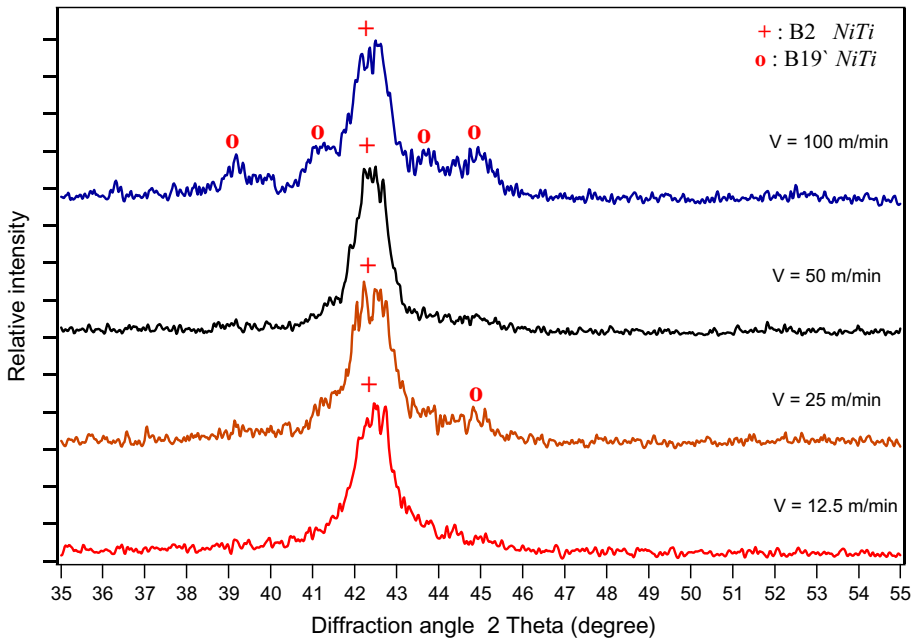

Fig. 7 XRD patterns of machined $Ni_{49.9}Ti_{50.1}$ SMAs with preheated condition

material cools down to room temperature, workpiece undergoes austenite-to-martensite transformation in some cases. It should be noted that in dry cutting, the materials were initially martensite, and transformation from martensite to austenite takes place during cutting, while in preheated case, the material was already austenite before the cutting process.

In both cases, austenite-to-martensite transformation during cooling is not complete or started so austenite phase is detected in machining-induced layers. The forward transformation in preheated conditions is started in some cases, thus, martensitic peaks appear in these condition.

Figure 8 shows XRD patterns of machined samples under cryogenic machining at selected cutting speeds. Reduced cutting speed results in broadening of the peaks in both conditions. It has been reported that deformation of martensite by cold deformation processes, such as cold rolling and equal channel angular extrusion, of NiTi results in peak broadening due to plastic strain, and the resulting dislocation density and defects (Ref 26-30). The present findings from cryogenic machining-induced XRD pattern agree with previous results where peak broadening after cutting, particularly at low speed, is observed.

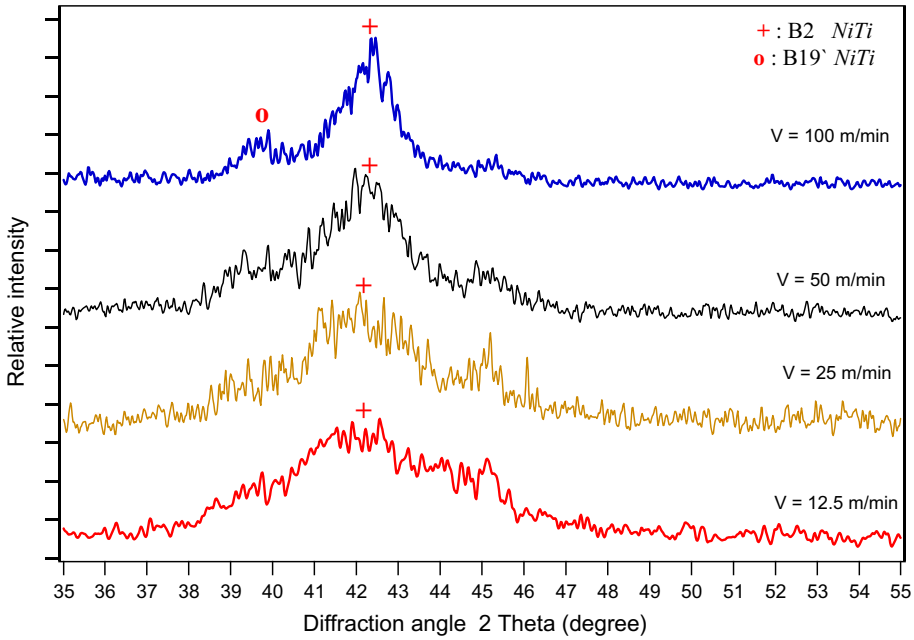

Fig. 8 XRD patterns of machined $Ni_{49.9}Ti_{50.1}$ SMAs with cryogenic cooling condition

In cryogenic cutting, the sample temperature was always below A_s (Ref 21), and thus, the cutting process significantly increased the dislocation density and resulted in stabilized martensite with the broadest peak at low speed. However, at high speeds, transformation from martensite to austenite was observed.

Overall, on the surface and subsurface of machined NiTi alloys under various conditions, phase transformation takes place resulting mainly from temperature and retained stress. Depending on cutting conditions, retained stress and plastic deformation completely or partially prevent the transformation from austenite to martensite or vice versa.

3.2 Phase Transformation Temperature of Machined Samples

DSC is a well-known tool for determining the phase transformation temperatures of SMAs (Ref 31). In this section, DSC results of machined samples and thus the effect of machining process of the phase transformation temperature at the surface layer of machined samples are discussed.

The DSC results at low (12.5 m/min) and high (100 m/min) cutting speeds were considered to reveal the effects of cutting speeds on the phase transformation temperatures under dry, preheated, and cryogenic cooling conditions. Austenite start (A_s) and austenite finish (A_f) temperatures of machine NiTi samples were examined and presented.

Figure 9 shows the DSC responses of the as-received and machined samples under different conditions. Peak broadening and increased transformation temperature are the typical response of machined samples obtained from this experimental study, as compared to as-received material. It is obvious that these two factors are affected from machining conditions and cutting parameters. Initial observation from DSC analysis clearly shows the effects of cryogenic machining on phase transformation behavior. Much broader peaks are resulting from cryogenic machining as compared to other conditions. Cryogenic machining at high speed highly altered the DSC response where double peaks and increased A_f are observed during heating. Dry machining also leads to obvious peak broadening and shifted transformation temperature at high-speed cutting process.

Figure 10 shows the phase transformation temperature of the surface layer of machined NiTi alloys. A_s (presented in red dash line) and A_f (presented in red line) of as-received material are 86 and 107 °C, respectively. The A_s and A_f of preheated and dry machined samples' surface layers are close to the transformation temperatures of the as-received material. A_f of cryogenically machined sample is approximately 136 °C at low speed and 138 °C at high speed. It is clear that transformation temperatures of cryogenically machined sample increased substantially with respect to all other machining conditions and as-received material.

Analysis from cold-rolling and deformation processes strongly corresponds with the findings resulting from the machining process results presented in the current study except under some conditions. Stabilized martensite state, via introducing residual stress and plastic strain due to extremely high dislocation density, (Ref 32) was much higher in the samples machined under cryogenic conditions. As a result, A_s and A_f of cryogenically machined samples were much higher than those in dry and preheated samples. In addition, the volume fraction of stabilized martensite decreased when dislocation density in the deformed material was reduced (Ref 33). Due to increased temperature in dry and preheated conditions, the volume fraction of stabilized martensite is much lower than in cryogenic machined samples. In some dry and preheated conditions, martensite stabilization does not take place because of very high cutting temperature which remarkably annihilated or reduced the dislocation density and resulted in forward transformation after machining process. This argument is well supported with XRD analysis, where in some conditions of dry and preheated samples, martensitic peaks were observed. Consequently, cryogenic machining leads to increasing transformation temperature in comparison with dry and preheated conditions.

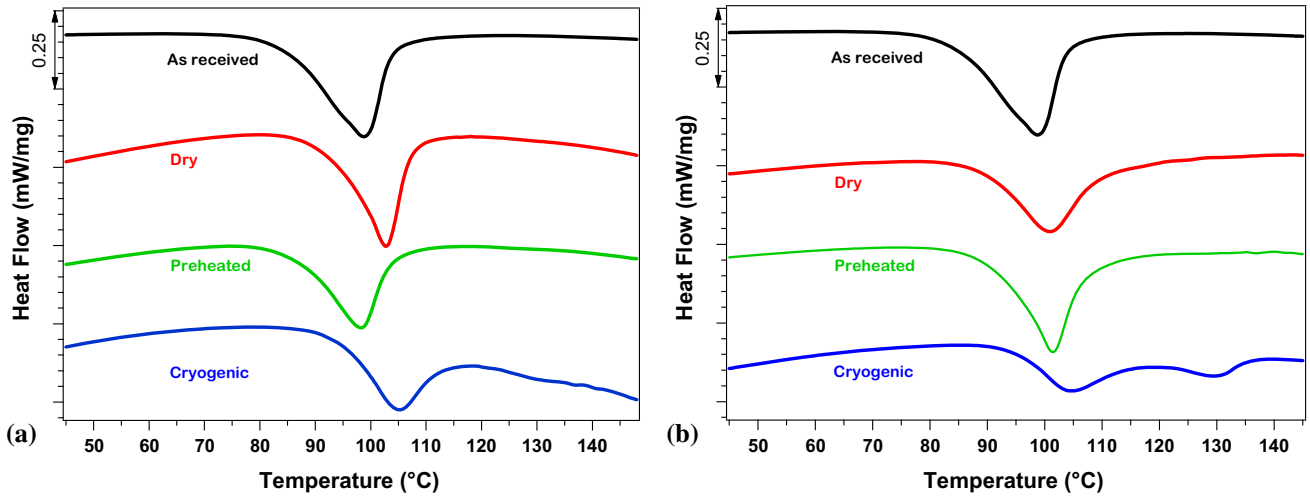

Fig. 9 DSC results of samples machined under different conditions at (a) 12.5 m/min, (b) 100 m/min cutting speed

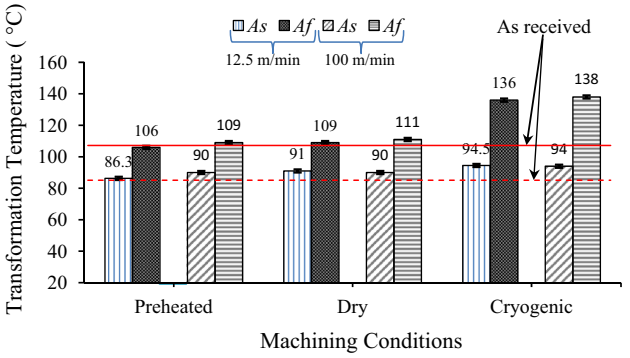

Fig. 10 Measured A_s and A_f temperatures as a function of different cutting conditions at 12.5 m/min cutting speed

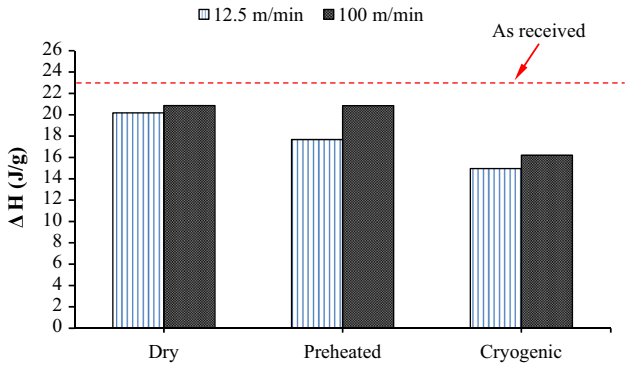

Fig. 11 Influence of machining conditions on latent heat of transformation for deformed layer of NiTi samples (Endothermic peak)

Observed increase in transformation temperatures resulting from the machining process can be due to the machining-induced martensite stabilization. Cryogenic machining remarkably increased the microhardness in the deformed layer (Ref 34). In addition, XRD analysis shows that cryogenically machined samples have substantial peak broadening. Other conditions show peak broadening at lower cutting speeds due to the residual stress and plastic strain introduced by machining. If heavier deformation takes place at high temperatures, the effect of deformation-induced stress relaxed to some extent, and the effect of deformation was limited in comparison with low-temperature cutting. In the literature, these phenomena have been shown as resulting from different processes, such as cold working processes (Ref 35). Researchers also report that the stabilization effect is observed as an increase in the critical temperature for the reverse transformation of the deformed martensite relative to the thermal martensite (Ref 36, 37). Mahmud et al. (Ref 35) also agreed that deformation-induced martensite stabilization in shape memory alloys is generally recognized as the increase of the transformation hysteresis via the increase in reverse transformation temperature (Ref 28, 35, 38). It was also noted that the magnitude of temperature increase is found to depend on several factors, including the deformation mode (Ref 39) and the level of deformation and alloy conditions (Ref 35, 36). According to Lin et al. (Ref 37), when cold-rolled specimens have been subjected to the reverse martensitic transformation of martensite to austenite, and then to the subsequent forward martensitic transformation of austenite to martensite, the deformed structures in the cold-rolled specimens mostly restored to the undeformed structure. The results indicate that the martensite stabilization is closely related to deformed structure induced by cold rolling (Ref 36, 37). Cold-rolled deformation can induce dislocation and vacancies (Ref 37). The deformed martensite structures and the deformation-induced dislocations/vacancies are expected to inhibit the reverse martensitic transformation by imposing a friction stress on the martensite/parent interface (Ref 37). Therefore, the reverse martensitic transformation temperatures, A_s and A_f, must shift to higher temperatures since transformation requires additional energy to overcome the friction stress (Ref 37). When the temperature was higher than A_f, the deformed martensite transformed to austenite phase and the deformed martensitic structure disappeared (Ref 28, 37).

Figure 11 illustrates the latent heat of transformation, ΔH, for the deformed layer of the samples extracted from the DSC curves. Latent heat of transformations for deformed layer of cryogenically machined sample at low and high cutting speeds are 14.9 and 16.2 J/g, respectively. The largest latent heat of transformation was measured with preheated and dry machined sample at high cutting speed was approximately 20.8 J/g. At low speed, the largest latent heat of transformation was measured in dry machined sample and followed by preheated

sample. These results show that machining conditions and cutting parameters influence the latent heat of transformation of the machined NiTi' surface and subsurface.

In cryogenic conditions, the latent heat of transformation, ΔH, was smaller than in dry and preheated conditions (Fig. 11). According to the literature, the drop in the ΔH values is attributed to the dislocations inhibiting the amount of material allowed to undergo the phase transformation (Ref 5, 40). Cryogenic machining resulted in higher dislocation density, which prevented the complete reverse transformation. Consequently, volume fraction of the material that undergoes transformation was smaller and, in turn, less energy was required.

Figure 12 shows the first and second cycle DSC responses of machined samples. It is obvious that there is a considerable difference in between the first and second cycles in terms of transformation temperature and peak broadening. Indeed, the largest difference in between the first and the second cycles occurs in cryogenically machined samples at either low or high cutting speed. Substantial recovery does occur at the second cycle in cryogenically machined samples. But, samples machined under dry and preheated conditions are also influenced when they are subjected to the second thermal cycle and their transformation temperatures get close to the transformation temperatures of the as-received material.

The current study's findings generally agree with the literature where thermal transformation reduces the effects of deformation where peaks get sharper and transformation temperatures decrease at the second cycle (Ref 37). However, not only increasing magnitude of temperature depends on deformation mode (Ref 39), but also decreasing rate of temperature and peak broadening after thermal cycling (second cycle) depend on the magnitude of residual stress, and plastic strain introduced via deformation process (in this case, machining process). This hypothesis is supported by the results shown in Fig. 12.

Although the effects of various bulk deformation process including cold forming, extrusion, and rolling, on the shape memory and phase transformation response of NiTi alloys are well investigated by researchers, the machining-induced shape memory and transformation response of the surface and subsurface of NiTi has not been systematically studied. This

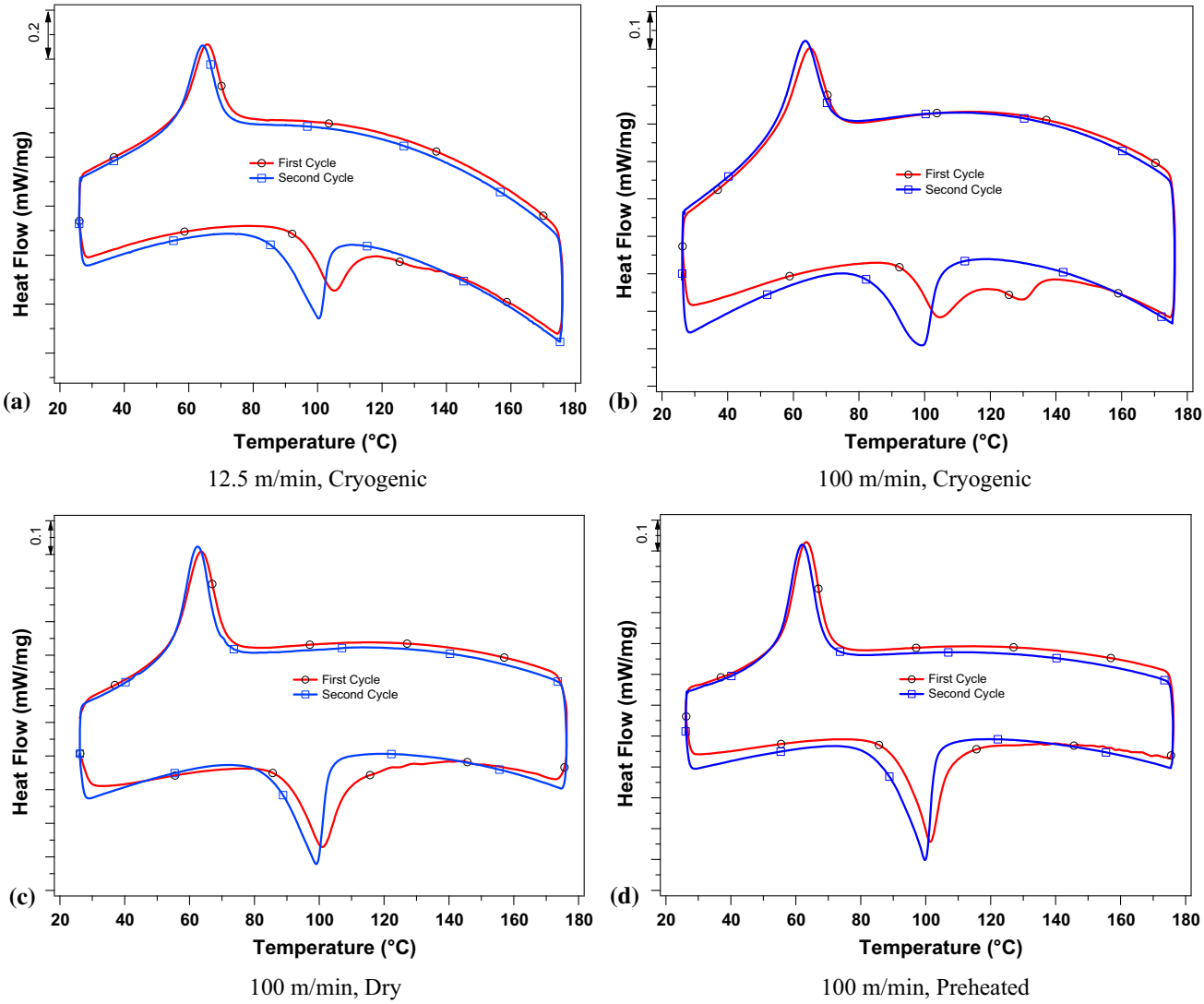

Fig. 12 DSC response of machined NiTi specimens at the first and second cycles, (a) 12.5 m/min cryogenically machined sample, (b) 100 m/min cryogenically machined sample (Ref 15), (c) 100 m/min dry machined sample (Ref 15), (d) 100 m/min preheated machined sample

study illustrates that machining process has potential to alter room temperature phase state and transformation temperatures of NiTi alloys. These changes can be visibly seen on the surface and subsurface of machined NiTi shape memory alloys. It is important to determine whether this altered structure can be utilized to enhance the performance of component made of NiTi alloy. Particularly in cases where machined NiTi is subjected to surface contact, then these newly created characteristics on the surface and subsurface can help to increase the wear and corrosion resistance. Thus, further investigation is needed to determine the effects of machining on the wear response of NiTi alloys.

4. Conclusions

The influence of various machining conditions and cutting speed on the phase state and the phase transformation response of NiTi shape memory alloys is presented in this paper. Following conclusions can be drawn from this study:

- Machining process has potential to alter room temperature phase of NiTi alloy. This change can be visibly seen on the surface and subsurface of machined NiTi shape memory alloy.
- Machining process effects phase state, phase transformation temperature and latent heat of transformation of the machined NiTi alloy. As this effect is seen on the surface and subsurface of machined parts, nonhomogeneous cross section in terms of shape memory properties occurs.
- Cryogenic machining has profound effect on phase state and phase transformation temperature of NiTi alloy as compared to other conditions (dry and preheating). It results in much broader peaks, larger transformation temperature. As compared to as-received material, cryogenic machining leads to approximately 27 and 29 percent increases in austenite finish temperature at low and high cutting speed, respectively.
- XRD analysis shows that complete transformation occurs in dry machining at all selected cutting speeds.
- As compared to latent heat for transformation of as-received material, machining process results in decreased latent heat for transformation. At low cutting speed, approximately 12, 23, and 35 percent reduction is measured at dry, preheated, and cryogenic machining, respectively. Increased cutting speed leads to slightly larger latent heat for transformation.
- After machining of NiTi material, heat treatment should be carried out to obtain homogeneous phase state and transformation temperature throughout the entire cross section of the NiTi sample.

Acknowledgments

Support from the NASA EPSCOR Program under Grant No. NNX11AQ31A and the NASA FAP Aeronautical Sciences Project are greatly acknowledged.

References

1. T. Baxevanis, A. Cox, and D. Lagoudas, Micromechanics of Precipitated Near-Equiatomic Ni-Rich NiTi Shape Memory Alloys, *Acta Mech.*, 2014, **225**, p 1–19
2. S.A. Shabalovskaya, On the Nature of the Biocompatibility and on Medical Applications of NiTi Shape Memory and Superelastic Alloys, *Biomed. Mater. Eng.*, 1996, **6**, p 267–289
3. S.A. Fadlallah, N. El-Bagoury, S.M. Gad El-Rab, R.A. Ahmed, and G. El-Ousamii, An Overview of NiTi Shape Memory Alloy: Corrosion Resistance and Antibacterial Inhibition for Dental Application, *J. Alloys Compd.*, 2014, **583**, p 455–464
4. K. Gall, J. Tyber, G. Wilkesanders, S.W. Robertson, R.O. Ritchie, and H.J. Maier, Effect of Microstructure on the Fatigue of Hot-Rolled and Cold-Drawn NiTi Shape Memory Alloys, *Mater. Sci. Eng. A*, 2008, **486**, p 389–403
5. D.A. Miller and D.C. Lagoudas, Thermomechanical Characterization of NiTiCu and NiTi SMA Actuators: Influence of Plastic Strains, *Smart Mater. Struct.*, 2000, **9**, p 640–652
6. J.A. Shaw and S. Kyriakides, Thermomechanical Aspects of NiTi, *J. Mech. Phys. Solids*, 1995, **43**, p 1243–1281
7. D.A. Miller and D.C. Lagoudas, Influence of Cold Work and Heat Treatment on the Shape Memory Effect and Plastic Strain Development of NiTi, *Mater. Sci. Eng. A Struct.*, 2001, **308**, p 161–175
8. Y. Kaynak, H. Karaca, R. Noebe, and I. Jawahir, Analysis of Tool-Wear and Cutting Force Components in Dry, Preheated, and Cryogenic Machining of NiTI, Shape Memory Alloys, *Procedia CIRP*, 2013, **8**, p 498–503
9. Y. Kaynak, H.E. Karaca, R.D. Noebe, and I.S. Jawahir, Tool-Wear Analysis in Cryogenic Machining of NiTi Shape Memory Alloys: A Comparison of Tool-Wear Performance with Dry and MQL Machining, *Wear*, 2013, **306**, p 51–63
10. K. Weinert and V. Petzoldt, Machining of NiTi Based Shape Memory Alloys, *Mater. Sci. Eng. A*, 2004, **378**, p 180–184
11. H.-C. Kim, J. Yum, B. Hur, and G.S.-P. Cheung, Cyclic Fatigue and Fracture Characteristics of Ground and Twisted Nickel-Titanium Rotary Files, *J. Endod.*, 2010, **36**, p 147–152
12. H. Huang, A study of High-Speed Milling Characteristics of Nitinol, *Mater. Manuf. Process.*, 2004, **19**, p 159–175
13. Y. Kaynak, H. Karaca, and I.S. Jawahir, Cryogenic Machining of NiTi Shape Memory Alloy, *6th International Conference and Exhibition on Design and Production of Machines and Dies/Molds*, 2011, p 23–26
14. Y. Kaynak, H. Tobe, R.D. Noebe, H. Karaca, and I.S. Jawahir, The Effects of Machining on Microstructure and Transformation behavior of NiTi Alloy, *Scr. Mater.*, 2014, **74**, p 60–63
15. Y. Kaynak, H. Karaca, and I.S. Jawahir, Surface Integrity Characteristics of NiTi Shape Memory Alloys Resulting from Dry and Cryogenic Machining, *Procedia CIRP*, 2014, **13**, p 393–398
16. Y. Kaynak, Machining and Phase Transformation Response of Room-Temperature Austenitic NiTi Shape Memory Alloy, *J. Mater. Eng. Perform.*, 2014, **23**, p 3354–3360
17. Y. Kaynak, H.E. Karaca, and I.S. Jawahir, Cutting Speed Dependent Microstructure and Transformation Behavior of NiTi Alloy in Dry and Cryogenic Machining, *J. Mater. Eng. Perform.*, 2015, **24**, p 452–460
18. A.P. Stebner, S.C. Vogel, R.D. Noebe, T.A. Sisneros, B. Clausen, D.W. Brown, A. Garg, and L.C. Brinson, Micromechanical Quantification of Elastic, Twinning, and Slip Strain Partitioning Exhibited by Polycrystalline, Monoclinic Nickel-Titanium During Large Uniaxial Deformations Measured via In-Situ Neutron Diffraction, *J. Mech. Phys. Solids,* 2013, **61**, p 2302–2330
19. O. Benafan, S.A. Padula, R.D. Noebe, T.A. Sisneros, and R. Vaidyanathan, Role of B19′ Martensite Deformation in Stabilizing Two-Way Shape Memory Behavior in NiTi, *J. Appl. Phys.*, 2012, **112**, p 093510–093511
20. K. Otsuka and X. Ren, Physical Metallurgy of Ti-Ni-Based Shape Memory Alloys, *Prog. Mater. Sci.*, 2005, **50**, p 511–678
21. Y. Kaynak, H.E. Karaca, R.D. Noebe, and I. Jawahir, The Effect of Active Phase of The Work Material on Machining Performance of a NiTi Shape Memory Alloy, *Metall. Mater. Trans. A*, 2015, **46**, p 2625–2636
22. V. Sharma and M. Pandey, Optimization of Machining and Vibration Parameters for Residual Stresses Minimization in Ultrasonic Assisted Turning of 4340 Hardened Steel, *Ultrasonics*, 2016, **70**, p 172–182

23. A. Thakur and S. Gangopadhyay, State-of-the-Art in Surface Integrity in Machining of Nickel-Based Super Alloys, *Int. J. Mach. Tools Manuf.*, 2016, **100**, p 25–54
24. Q. Wang and Z. Liu, Plastic Deformation Induced Nano-Scale Twins in Ti-6Al-4V Machined Surface with High Speed Machining, *Mater. Sci. Eng. A*, 2016, **675**, p 271–279
25. G. Rotella, O.W. Dillon, Jr., D. Umbrello, L. Settineri, and I.S. Jawahir, The Effects of Cooling Conditions on Surface Integrity in Machining of Ti6Al4V Alloy, *Int. J. Adv. Manuf. Technol.*, 2014, **71**, p 47–55
26. B.D. Cullity and S.R. Stock, *Elements of X-Ray Diffraction*, Prentice Hall, Upper Saddle River, 2001
27. M.E. Mitwally and M. Farag, Effect of Cold Work and Annealing on the Structure and Characteristics of NiTi Alloy, *Mater. Sci. Eng. A*, 2009, **519**, p 155–166
28. I. Karaman, H.E. Karaca, Z. Luo, and H. Maier, The Effect of Severe Marforming on Shape Memory Characteristics of a Ti-Rich NiTi alloy Processed Using Equal Channel Angular Extrusion, *Metall. Mater. Trans. A*, 2003, **34**, p 2527–2539
29. H. Shahmir, M. Nili-Ahmadabadi, M. Mansouri-Arani, and T.G. Langdon, The Processing of NiTi Shape Memory Alloys by Equal-Channel Angular Pressing at Room Temperature, *Mater. Sci. Eng. A*, 2013, **576**, p 178–184
30. D.N.A. Shri, K. Tsuchiya, and A. Yamamoto, Surface Characterization of TiNi Deformed by High-Pressure Torsion, *Appl. Surf. Sci.*, 2014, **289**, p 338–344
31. J. Uchil, F. Fernandes, and K. Mahesh, X-Ray Diffraction Study of the Phase Transformations in NiTi Shape Memory Alloy, *Mater. Charact.*, 2007, **58**, p 243–248
32. S. De la Flor, C. Urbina, and F. Ferrando, Effect of Mechanical Cycling on Stabilizing the Transformation Behaviour of NiTi Shape Memory Alloys, *J. Alloys Compd.*, 2009, **469**, p 343–349
33. J. Olbricht, A. Yawny, A. Condó, F. Lovey, and G. Eggeler, The Influence of Temperature on the Evolution of Functional Properties During Pseudoelastic Cycling of Ultra Fine Grained NiTi, *Mater. Sci. Eng. A*, 2008, **481**, p 142–145
34. Y. Kaynak, Process-Induced Surface Integrity in Machining of NiTi Shape Memory Alloys, University of Kentucky. Ph.D. Dissertation (2013)
35. A.S. Mahmud, H. Yang, S. Tee, G. Rio, and Y. Liu, Effect of Annealing on Deformation-Induced Martensite Stabilisation of NiTi, *Intermetallics*, 2008, **16**, p 209–214
36. Y. Liu and D. Favier, Stabilisation of Martensite Due to Shear Deformation via Variant Reorientation in Polycrystalline NiTi, *Acta Mater.*, 2000, **48**, p 3489–3499
37. H. Lin, S. Wu, T. Chou, and H. Kao, The Effects of Cold Rolling on the Martensitic Transformation of an Equiatomic TiNi Alloy, *Acta Metall. Mater.*, 1991, **39**, p 2069–2080
38. Y. Liu and Z. Xie, Detwinning in Shape Memory Alloy, *Progress in Smart Materials and Structures*, P.L. Reece, Ed., Nova Science Publishers Inc, NY, 2007, p 29–65
39. G. Tan and Y. Liu, Comparative Study of Deformation-Induced Martensite Stabilisation via Martensite Reorientation and Stress-Induced Martensitic Transformation in NiTi, *Intermetallics*, 2004, **12**, p 373–381
40. J.T. Lim and D.L. McDowell, Degradation of an Ni-Ti Alloy During Cyclic Loading, *1994 North American Conference on Smart Structures and Materials*, International Society for Optics and Photonics, 1994, p 326–341